Investigation of an Intensifying-flux Variable Flux-leakage Interior Permanent Magnet Machine for Wide Speed Range

Xiping Liu, Dabin Liu, Siting Zhu, and Jianwei Liang

***Abstract*—In this paper, a novel intensifying-flux variable flux-leakage interior permanent magnet (IFVF-IPM) machine is proposed, in which flux barriers were designed deliberately between the adjacent poles to obtain intensifying-flux effect and variable flux-leakage property. The rotor topology and design principles of the proposed machine are also introduced. Then, a multi-objective optimization method is adopted based on the sensitivity analysis, and some design variables of IFVF-IPM machine with strong sensitivity are selected to optimization progress by using the non-dominated sorting genetic algorithm-II (NSGA-II). Moreover, the electromagnetic characteristics of conventional IPM machine, conventional IFVF-IPM machine (CIFVF-IPM) and the novel IFVF-IPM machine are compared based on the finite element analysis (FEA) method which includes flux linkage, inductances characteristic, torque-speed envelops and power characteristic, as well as evaluation of the risk of irreversible demagnetization. Finally, the experiment results show that the IFVF-IPM machine has a better performance in flux weakening capability for wide speed range and a lower risk of irreversible demagnetization, which indicates the validity and feasibility of the proposed machine.**

***Index Terms*—Interior permanent magnet (IPM) machine, Intensifying-flux, Variable flux-leakage, Electromagnetic performance, Demagnetization, Finite element analysis (FEA), Wide speed range.**

I. INTRODUCTION

INTERIOR permanent magnet synchronous machines (IPMSM) have the characteristics of high torque density and high efficiency, which is widely used in electric vehicles and hybrid vehicles[1]. Due to the internal magnetic field of the conventional IPMSM is difficult to regulate, and to achieve a wide range of speed regulation, a flux weakening regime has to be utilized to inject a negative d-axis current to weaken the air gap magnetic field and suppress the back-EMF while operating within inverter capacity [2], [3]. However, large negative d-axis current will increase the risk of demagnetization of permanent magnets (PMs) and copper loss, and this issue is addressed by intensifying-flux interior permanent magnet (IF-IPM) machine with an innovative rotor topology which characterized L_d>L_q to an extent in reference [3]. And because of the above inductance characteristic of IF-IPM machine, when maximum torque per ampere (MTPA) control strategy is used below the base speed, the MTPA operating point trajectory is in the first quadrant, and the positive d-axis current will obtain positive reluctance torque, then the d-axis current changes from positive to negative in flux weakening region particularly [2]. Compared with the conventional IPM machine, whose d-axis current is always negative, d-axis current in IF-IPM machine which is relatively smaller can reduce the risk of irreversible demagnetization of the permanent magnet, and a larger L_d also can help broaden the speed range at the same time.

Recently, lots of scholars are making investigations on IF-IPM machines which have special rotor topology. A novel IF-IPM machine with special rotor topology is proposed in [4], different types of flux barriers on the q-axis are set up in the rotor, and it is concluded that the surface flux barrier is a more reasonable method to achieve the intensifying-flux effect. In [5], an intensifying-flux permanent magnet brushless machine with two-layer segmented permanent magnets is proposed, and two machines with the characteristic of L_d>L_q are proposed and compared in [6], with the evaluation of the risk of irreversible demagnetization of the machine in [6]. Particularly, an IF-IPM machine in reference [7] has the excellent performance in efficiency and self-sensing, and the design is evaluated by finite element analysis methods.

Based on the research status on IF-IPM machine, many scholars have proposed IF-IPM machines with the characteristic of variable flux-leakage [8]-[11]. In this kind of machine, flux-leakage paths are deliberately set up, and the q-axis current is reduced to obtain a flux weakening ability when operating in the flux weakening region, thereby broadening the speed regulation range. This kind of unique structural rotor design can increase the output power when the machine is operating at high speed, and reduce the iron loss under the condition of high speed and low torque [8]. And a new segmented IPMSM is also designed for a wide speed range in [12], in which the negative d-axis current is used to canalize rotor flux into rotor bridges, the air-gap flux linkage and back-EMF can be weakened in this way which are being well regulated over a wide speed range.

In this paper, we present a special rotor design with

Manuscript received October 27, 2021; revised January 28, 2022; accepted February 28, 2022. date of publication June 25, 2022; date of current version June 18, 2022.

This work was supported in part by the National Natural Science Foundation of China under grant no.52067008. *(Corresponding Author: Dabin Liu)*

Xiping Liu, Dabin Liu, Siting Zhu and Jianwei Liang are with School of Electrical Engineering and Automation, Jiangxi University of science and technology, Ganzhou 34100, China (827552570@qq.com)

Digital Object Identifier 10.30941/CESTEMS.2022.00028

flux-leakage paths to obtain a variable flux-leakage property based on an IF-IPM machine, and the electromagnetic characteristics of the intensifying-flux variable flux-leakage (IFVF-IPM) machine will be evaluated by finite element analysis (FEA) method. It expects that the proposed machine has the characteristic of variable flux-leakage, which can expand output power at high speeds, achieve a wide range of speed regulation, less core loss and reduce the risk of demagnetization compared with conventional IPM machines.

II. Motor Topology and Operating Principles

To clarify the differences between the conventional IPM machine and the IFVF-IPM machine more suitably and reasonably and evaluate the performance of the proposed IFVF-IPM machine convincingly, a conventional IPM motor is introduced as a comparison. The rotor topologies of the two machines are shown in Fig 1. Fig.1(a) shows an example of conventional IPM machine with 48 slots 8 poles, in which the PMs are designed to be thin in general. Fig.1(b) shows the proposed IFVF-IPM machine which increases the reluctance of the q-axis by setting up flux barriers and thus results in the characteristic of L_d>L_q. And the following describes the characteristics of the proposed IFVF-IPM machine from intensifying-flux effect and magnetic circuit design.

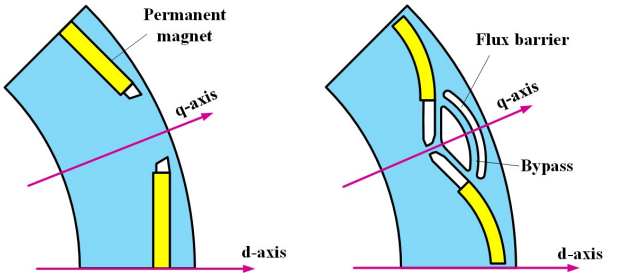

Fig. 1. Configurations of the two machines. (a) Conventional IPM machine. (b) IFVF-IPM machine.

A. Feasible Design for Intensifying-flux Effect

The IF-IPM machine is a novel type machine and the intensifying-flux effect is achieved through the special design of rotor topology. The large d-axis inductance is conducive to enhance the ability of flux weakening. Fig.1(b) shows the rotor topology of the proposed IFVF- IPM machine, in which the characteristic of L_d>L_q can be generated by increasing the permeance of d-axis while reducing the permeance of q-axis by the following relationship:

$$L = N^2 \Lambda \tag{1}$$

where L is the inductance in *d-q* coordinate system; and N, Λ represent the number of winding-turns and permeance. The IFVF-IPM machine reduces the permeance of q-axis by setting a multi-layer flux barriers on the q-axis, and a segmented structure is adopted in PMs to increase the permeance of d-axis to achieve L_d>L_q. In IPMSM, the maximum speed which IFVF-IPM machine can achieve is:

$$n_{max} = \frac{60 U_{lim}}{2\pi p \left| \psi_f - L_d I_{lim} \right|} \tag{2}$$

in which n_{max}, U_{lim}, I_{lim}, ψ_f and p are stand for the maximum rotation speed, the limiting voltage and current, pairs of poles, flux linkage of PMs, respectively. According to equ. (2), it can be judged that the smaller flux linkage of PMs also can help to expand the range of speed regulation.

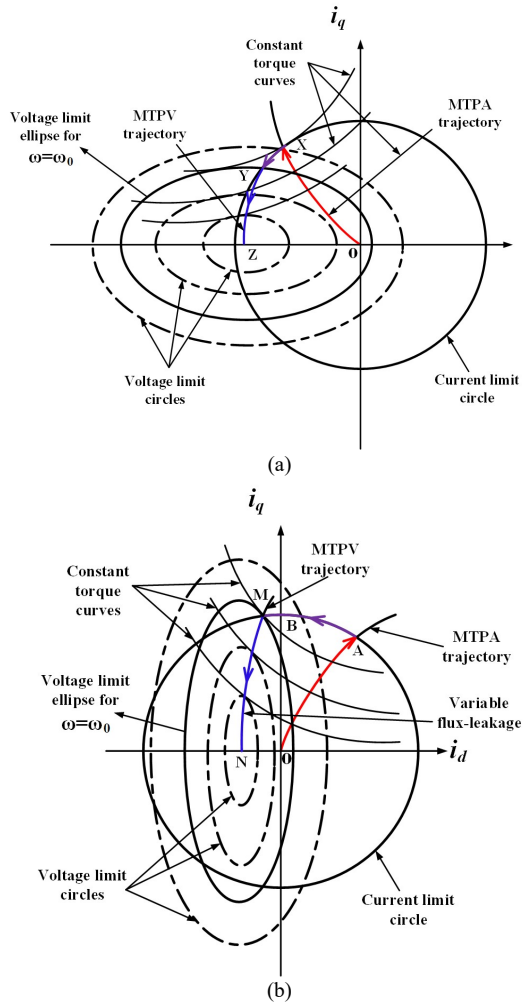

Fig. 2. Operating point trajectory of the two machines (a) Conventional IPM machine. (b) IFVF-IPM machine.

The preliminary research shows that under the MPTA control strategy, negative d-axis current is used in conventional IPM machine to generate negative reluctance torque even in the flux weakening region and the operating point is always maintained in the second quadrant as displayed in Fig.2(a). On the contrary, as shown in Fig.2(b), because of the characteristic of L_d>L_q in IFVF-IPM machine, the MTPA trajectory is in the first quadrant of the (i_d,i_q) plane from point O to A, which cause positive d-axis current produces positive reluctance torque and improves the overall output torque below the based speed with heavy load. Then, the current of d-axis begins to move closer to the second quadrant while PM flux is constant from point A to B. And point M is in the second quadrant of (i_d,i_q) plane as is seen where the PM flux is varying with the negative d-axis current from B to M, after that the voltage limit ellipse shrinks. During the shrinking of the voltage ellipse, the q-axis component of current is also constantly decreasing, which will result a larger flux-leakage and make the PM flux weaker which can maximum n_{max} according to equ. (2). In some way, the d-axis current of the IFVF-IPM machine is always

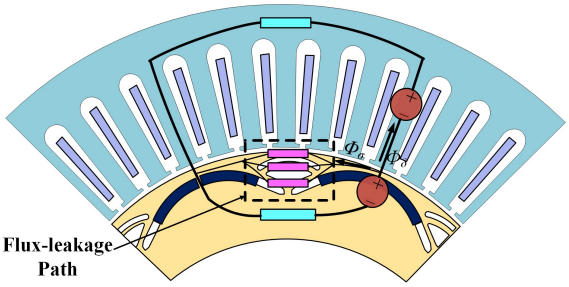

Fig. 3. Schematic drawing of magnetic circuits for the IFVF-IPM machine.

relatively small compared with the conventional IPM machine during operation progress, and the risk of irreversible demagnetization can be significantly reduced.

B. Magnetic Circuit Design for IFVF-IPM Machine

To ensure the maximum utilization of PMs, flux barriers are adopted to minimize the flux leakage in conventional IPM machine. But as for the IFVF-IPM machine, a flux leakage path was designed deliberately between the adjacent poles as shown in Fig. 3, and the flux leakage is generally designed to be large when operating in light load conditions especially. In this way the PM flux linkage is reduced, which is beneficial to reduce the back EMF and iron loss.

With the increase of the q-axis current, the flux leakage path between the adjacent poles tends to be saturated, and the flux leakage is passively reduced to zero, which can meet the needs for high load condition. The process of variable flux-leakage is shown in Fig. 2(b).

If the magnetic equivalent circuit of Fig. 4 is used, the boundary conditions for the realization of flux-leakage characteristics can be simply derived in equ. (3)-(6):

$$\begin{bmatrix}\Phi_\delta\\ \Phi_m\end{bmatrix}=\frac{1}{det\,R}\begin{bmatrix}R_{ro}+R_{b1}\parallel R_{b2}\parallel R_{b3} & R_{b1}\parallel R_{b2}\parallel R_{b3}\\ R_{b1}\parallel R_{b2}\parallel R_{b3} & R_{st}+R_{ag}+R_{b1}\parallel R_{b2}\parallel R_{b3}\end{bmatrix}\begin{bmatrix}NI_{st}\\ F_{pm}\end{bmatrix} \tag{3}$$

$$det\,R=\left(R_0+R_{b1}\parallel R_{b2}\parallel R_{b3}\right)\left(R_{st}+R_{ag}+R_{b1}\parallel R_{b2}\parallel R_{b3}\right)-\left(R_{b1}\parallel R_{b2}\parallel R_{b3}\right)^2 \tag{3}$$

where Φ_m is magnet flux leakage;

Φ_δ represents magnet flux in the stator side;

Φ_σ stands for flux leakage.

R_x is reluctance.

For a reliable flux leakage circuit, it is necessary to control the flux-leakage to 0 by the controlled armature current on the stator side, then:

$$\Phi_m-\Phi_\delta=0 \tag{4}$$

As a result:

$$\frac{NI_{st}}{F_{pm}}\geq\frac{R_{ag}+R_{st}}{R_{ro}} \tag{5}$$

In which I_{st} stand for armature current, F_{pm} is magnetomotive force, Φ and R represent magnetic flux and reluctance.

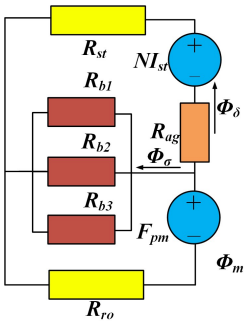

Fig. 4. Magnetic equivalent circuit.

From the equ. (6), we can see that whether it is in the process of variable flux leakage is mainly determined by the magnetomotive force on the stator side. If the armature current of q-axis is continuously increased, the magnetic flux leakage circuit will tend to be saturated, and the flux leakage path area reaches deep magnetic saturation when the armature current of q-axis is large enough, and the armature current will no longer cause the flux leakage vary at the meanwhile. Therefore, the flux leakage can be controlled by controlling the q-axis component of current when the flux leakage path is not saturated, which means the air gap flux can be adjusted. In addition, the arc-shaped permanent magnet can maximize the flux leakage of the proposed machine because of the special magnetization direction, and the flux leakage path will eventually become saturated, thus this innovative design can increase the rate of change of controllable flux leakage without sacrificing too much output torque.

III. Design Optimization

Based on the above design and analysis of the IFVF-IPM machine, and to make the proposed IFVF-IPM machine have the optimal performance, it is necessary to optimize the rotor topology of the proposed IFVF-IPM machine [13],[14]. Firstly, the optimization objectives are determined. Secondly, the parameterized model of the IFVF-IPM machine is needed to be established as shown in Fig. 5, and the design variables and the corresponding constraint are also determined simultaneously.

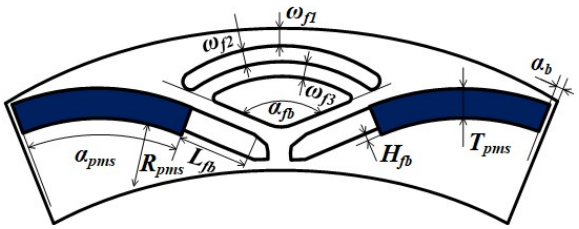

Fig. 5. Parameterization of the proposed IFVF-IPM rotor structure.

Then, the parameterized model is subjected to sensitivity analysis on optimization objectives, so the design variables are divided into sensitive layers and insensitive layers according to comprehensive sensitivity index to improve the efficiency and accuracy of the algorithm. Finally, the design variables in sensitive layer are selected to optimize by multi-objective algorithm NSGA-II to obtain the most excellent design.

A. Optimization Objectives:

The direct optimization objectives are as follows:

(1) Maximizing average torque using MTPA method T_{avg}.
(2) Minimizing torque ripple T_{ripple}.
And torque ripple is generally defined as:

$$T_{ripple}=\frac{T_{\max}-T_{\min}}{T_{avg}}\times 100\% \tag{7}$$

where T_{max} and T_{min} are the maximum and minimum values of torque.
(3) Maximizing reverse saliency ratio K_{rs}, which can be defined as:

$$K_{rs}=\frac{L_d}{L_q} \tag{8}$$

And the indirect optimization objectives are as follows:
(1) Variable flux range γ, which is not a direct optimization objective but also should be considered carefully.
(2) Inductance characteristics.

B. Design Parameters of the IFVF-IPM Machine

According to the operation principle of the IFVF-IPM machine, some parameters are chosen as design variables. And Table I lists the selected design variables and variation ranges of the parameterized model of IFVF-IPM machine.

TABLE I
DESIGN VARIABLES AND VARIATION RANGES

Design variables	Variation Ranges
α_{pms}	[41deg,50deg]
α_b	[0.8deg,2.5deg]
α_{fb}	[55deg,68deg]
ω_{f1}	[1.2mm,2mm]
ω_{f2}	[1.2mm,2mm]
ω_{f3}	[1.2mm,2mm]
H_{fb}	[0.8mm,1.5mm]
T_{pms}	[2.8mm,3.6]
R_{pms}	[19mm,22mm]
L_{fb}	[6mm,9mm]

C. Sensitivity Analysis

In the design process of the IFVF-IPM machine, each design variables has a different degree of influence on the optimization objectives. Hence, the sensitivity analysis of design variables on the optimization objectives are necessary. And the result of sensitivity analysis on all the design variables are shown in Fig.6, in which the greater amplitude of $S(x_i)$ means a greater impact on optimization objectives. The sensitivity index $S(x_i)$ can be written as:

$$S(x_i)=\frac{V(E(y/x_i))}{V(y)} \tag{9}$$

In which $E(y/x_i)$ represents average value of optimization objective y when x_i is constant. $V(E(y/x_i))$ is variance of $E(y/x_i)$ when $V(y)$ is variance of y. Then, a comprehensive sensitivity analysis is adopted which can reduce the parameter dimension to increase the efficiency and accuracy of the algorithm, and the function is defined as:

$$S_{IFVF-IPM}(x_i)=\lambda_t|S_t(x_i)|+\lambda_r|S_r(x_i)|+\lambda_{rs}|S_{rs}(x_i)| \tag{10}$$

where $|S_t(x_i)|$, $|S_r(x_i)|$ and $|S_{rs}(x_i)|$ are the absolute value of $S(x_i)$ to T_{avg}, T_{ripple} and K_{rs}, and λ_t, λ_r and λ_{rs} are the weight coefficient of T_{avg}, T_{ripple} and K_{rs} which can be designed by requirement.

According to (10), the comprehensive sensitivity analysis can be calculated as shown in Table II.

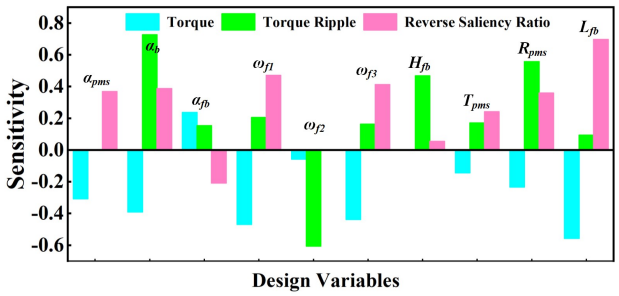

Fig. 6. Result of sensitivity analysis.

TABLE II
WEIGHT COEFFICIENT AND COMPREHENSIVE SENSITIVITY INDEX

Variables	Optimization objectives			Comprehensive sensitivity index
	$S_t(x_i)$ λ_t=0.4	$S_r(x_i)$ λ_r=0.3	$S_{rs}(x_i)$ λ_{rs}=0.3	
α_{pms}	-0.3073	0	0.3687	0.23353
α_b	**-0.3902**	**0.7277**	**0.3877**	**0.4907**
α_{fb}	0.2365	0.1544	-0.208	0.20332
ω_{f1}	**-0.4691**	**0.2055**	**0.4719**	**0.39086**
ω_{f2}	-0.0568	-0.605	0	0.20422
ω_{f3}	**-0.4375**	**0.1629**	**0.4125**	**0.34762**
H_{fb}	0	0.4682	0.0554	0.15708
T_{pms}	-0.1436	0.1718	0.2421	0.18161
R_{pms}	**-0.233**	**0.5571**	**0.3604**	**0.36845**
L_{fb}	**-0.5559**	**0.0941**	**0.6969**	**0.45966**

D. Optimization With the Sensitive Parameters

According to the calculation results in Table II, the design variables with comprehensive sensitivity $S_{IFVF-IPM}(x_i)$>0.3 are selected as sensitive design variables, and the rest are selected as insensitive design variables, as shown in Table III. Then, the objective optimization function of the proposed IFVF-IPM machine is as follows:

$$f(x_j)_{min}=\lambda_t\frac{T'_{avg}(x_j)}{T_{avg}(x_j)}+\lambda_r\frac{T'_{ripple}(x_j)}{T_{ripple}(x_j)}+\lambda_c\frac{K'_{rs}(x_j)}{K_{rs}(x_j)} \tag{11}$$

Where, min $x_j\le x_j\le$max x_j, j=1,2,3,4,5. $T'_{avg}(x_j)$, $T'_{ripple}(x_j)$ and $K'_{rs}(x_j)$ are initial values of average torque, torque ripple and cogging torque respectively. $T_{avg}(x_j)$, $T_{ripple}(x_j)$ and $K_{rs}(x_j)$ are optimal values of average torque, torque ripple and reverse saliency ratio respectively. And the boundary constraint of IFVF-IPM motor is:

$$T_{avg}\ge 50N;\ T_{ripple}\le 15\%;\ K_{rs}\ge 1 \tag{12}$$

Then, NSGA-II is adopted in the optimization process. The optimization results are shown in Fig. 21, and the optimal point has been marked.

Finally, the final determined values of the key design variables are listed in Table IV.

TABLE III
STRATIFICATION OF THE DESIGN VARIABLES

Classification	Selected parameters
Sensitive	**α_b, ω_{f1}, ω_{f3}, R_{pms}, L_{fb}**
Insensitive	α_{pms}, α_{fb}, ω_{f2}, H_{fb}, T_{pms}

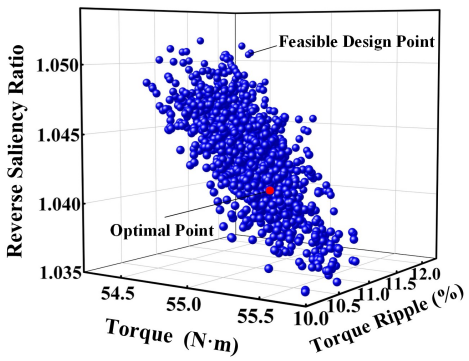

Fig. 7. Results of optimization.

TABLE IV
OPTIMIZATION RESULTS OF PROPOSED IFVF-IPM MACHINE

VLF-IPM motor		Initial values	Optimal values
Design variables	α_b	68 deg.	67.4 deg.
	ω_{f1}	2 mm	1.2 mm
	ω_{f3}	2 mm	1.2 mm
	R_{pms}	21 mm	21.8 mm
	L_{fb}	9 mm	8.8 mm
Optimization objectives	T_{avg}	48.5N·m	55.6 N·m
	T_{ripple}	13.7%	10.4%
	K_{rs}	1.48	1.04
	γ	40.9%	26.4%

IV. ELECTROMAGNETS PERFORMANCES ANALYSIS

To evaluate the validity of the proposed IFVF-IPM machine design reasonably and suitably, the conventional IFVF-IPM (CIFVF-IPM) machine is introduced here, both machines have the same volume of PMs. And the differences between two machines are that proposed IFVF-IPM machine has 3 parallel leakage flux paths, which can achieve a larger variable flux range, and arc-shaped PMs is also adopted. And the finite element analysis (FEA) method is used to for the further analysis. The main parameters of the two machines are shown in Table Ⅴ.

TABLE V
KEY PARAMETERS OF THE CIFVF-IPM MACHINE AND IFVF-IPM MACHINE

Design variables/units	CIFVF-IPM machine	Proposed IFVF-IPM machine
Stator Outer Diameter/mm	269.9	269.9
Rotor Outer Diameter/mm	110.6	110.6
Length/mm	40	40
Air-gap Length/mm	0.9	0.9
Rated Speed/rpm	1000	1000
Rater Phase Current/A	48	48
Number of Turns	15	15
Volume of PMs per Pole/cm^3	5.84	5.84

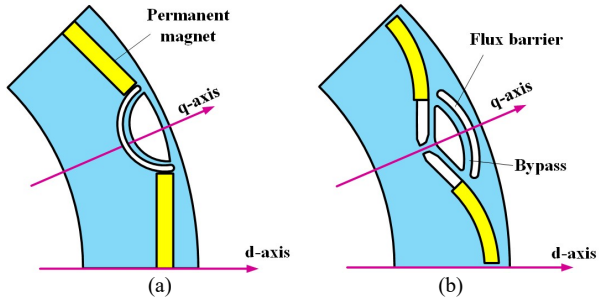

Fig. 8. Configurations of the two IFVF-IPM machines. (a) CIFVF-IPM machine. (b) IFVF-IPM machine.

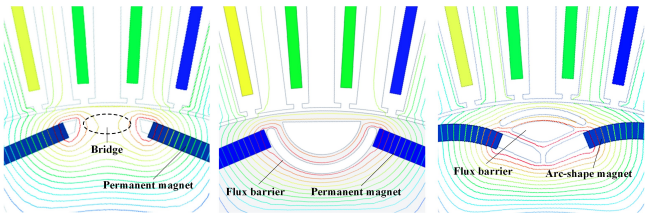

Fig. 9. Variable flux leakage property of no load (a) Conventional IPM machine (b) CIFVF-IPM machine (c) IFVF-IPM machine

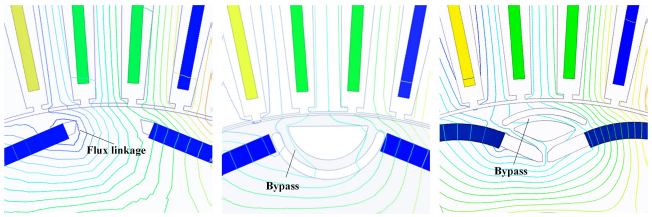

Fig. 10. Variable flux leakage property of loaded condition (a) Conventional IPM machine (b) CIFVF-IPM machine (c) IFVF-IPM machine

A. Comparison of Flux Linkage

As shown in Fig. 9(a), which is the distribution of flux lines of the conventional IPM machine under no-load condition. Within the allowable range of the stress conditions, the flux barriers at both ends of the magnetic poles should be as close as possible to the edge of the rotor to reduce the width of the flux leakage path to minimize the flux leakage generally, and therefore flux leakage would be small under working conditions, as shown in Fig.10(a). To obtain the ideal variable flux leakage property for two IFVF-IPM machines, the width of bypass between flux barriers needs to be set reasonably, and inductance of q-axis is also influenced by the flux barriers which has an impact on the formation of intensifying-flux effect. As is seen in Fig.9(b) and Fig.9(c), a large amount of flux leakage surges into the flux leakage bypass and flows into the adjacent magnetic poles under no-load condition, and Fig.10(b) and Fig.10(c) show that the flux passes through the air gap to the stator side instead of the flux leakage path under the rated working condition, which reflects that the flux leakage path is saturated and the flux leakage is minimized.

The FEA result shows that d-axis flux linkage varies with the armature current of q-axis in Fig.11. When the current of q-axis is small, the saturation degree of the flux leakage circuit is low, so the leakage flux is large which leads to the small flux linkage of d-axis. The flux leakage circuit tends to be deeply saturated when the armature current of q-axis exceeds 48A. The variable flux range of proposed IFVF-IPM machine is wider than CIFVF-IPM machine, 26.4% and 14.1%, respectively.

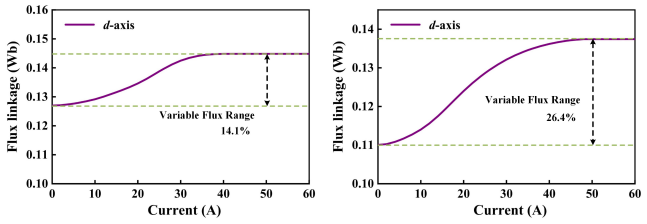

Fig. 11. Relationship between i_q and flux linkage of d-axis. (a)CIFVF-IPM machine. (b) IFVF-IPM machine

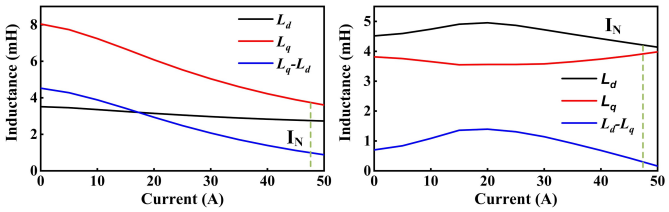

Fig. 12. Inductance characteristics of the two machines. (a) Conventional IPM machine. (b) IFVF-IPM machine

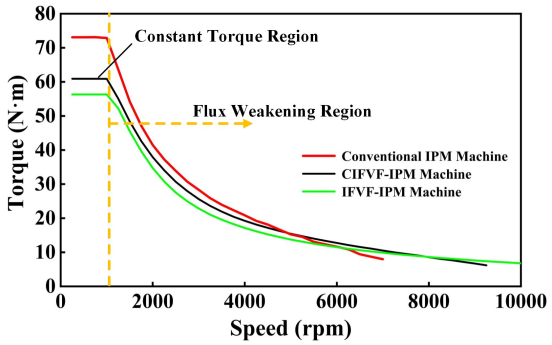

Fig. 13. Torque-speed envelops for three machines.

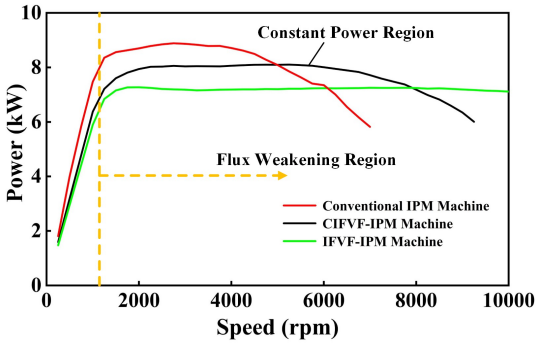

Fig. 14. Power-speed envelops for three machines.

B. *Inductance Characteristics*

The inductance characteristic is essential for performance of the IFVF-IPM machine. It can be known from the equ. (2) that it is influential on the flux weakening ability and wide-range speed regulation. Fig. 12 depicts L_d and L_q at different current condition. Fig.12(a) shows that L_q is always greater than L_d in conventional IPM machine, and the value of L_d is not sensitive to the armature current. While Fig.12(b) describe the L_d of the proposed IFVF-IPM machine is always greater than L_q, which is a significant feature of the intensifying-flux effect.

C. *Torque-speed Envelope and Power Characteristic*

The main advantage of the proposed machine is wide speed range, and the torque-speed envelopes and power-speed envelopes of conventional IPM machine, the CIFVF-IPM machine and the optimal IFVF-IPM machine are shown in Fig.13 and Fig.14. From Fig.13, conventional IPM machine has a better performance of output torque among the three machine in the constant torque region, but when in the flux weakening region, the torque of the conventional IPM machine drops faster, and the output torque is lower than the 10% of the rated torque when the rotation speed reaches 7000r/min, which the speed expansion range reaches 1:7, while the speed of the

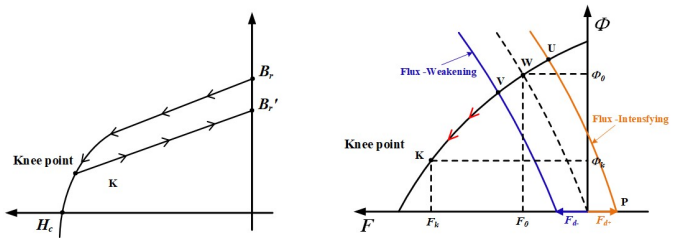

Fig. 15. Demagnetization principle of PMs (a)B-H curve (b)PMs at different operation states.

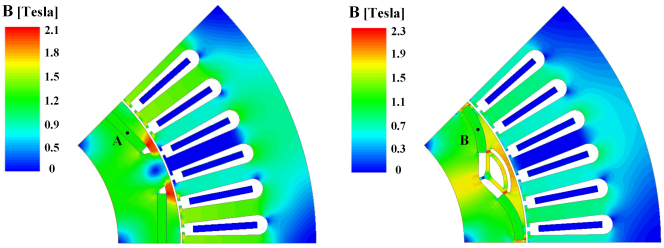

Fig. 16. Flux density distributions under no load (a) Conventional IPM machine. (b) IF-VF IPM machine.

IFVF-IPM machine reaches 10000r/min in flux weakening region which means achieving a wider range of speed regulation. The output power-speed envelops is shown in Fig.10, and the output power curve of IFVF-IPM machine is flatter and the constant power range is wider compared with the conventional IPM machine and the CIFVF-IPM machine.

D. *Evaluation the Irreversible Demagnetization Risk of PMs*

High temperature, high frequency vibration, corrosion, and strong current, etc., or combined effects may cause the demagnetization of the PMs, and the overload current is always the most frequent factor that causes the phenomenon. At present work, we use the FEA method to evaluate the risk of irreversible demagnetization of PMs in the case of deep demagnetization or strong overload current in the IFVF-IPM machine and conventional IPM machine.

The schematic diagram of the demagnetization principle of the PMs of the two machines are shown in the Fig.15. In Fig.15(a), when the magnetic force recovery line runs below the knee point, the PMs cannot recover according to the original B-H curve from K to Br but the new curve from K to Br' which means which means the PMs have undergone irreversible demagnetization. It is depicted the trajectory of the operating points states of the two mateines in different operating region in Fig.15(b). For the conventional IPM machine, the operating point moves from W to V, and then enters the flux weakening region while it is easy to cause demagnetization if the negative d-axis current is too large. But for IFVF-IPM machine, due to the positive inductance of d-axis, its operating point transferred from U to W firstly, and then gradually enters the flux weakening region toward V, which greatly reduces the risk of PMs of irreversible demagnetization.

The no-load flux density cloud maps of the two machines are shown in Fig.16, respectively, where A and B are selected as the observation points of the PMs flux density. Here, the rated current and twice the rated current under the condition of

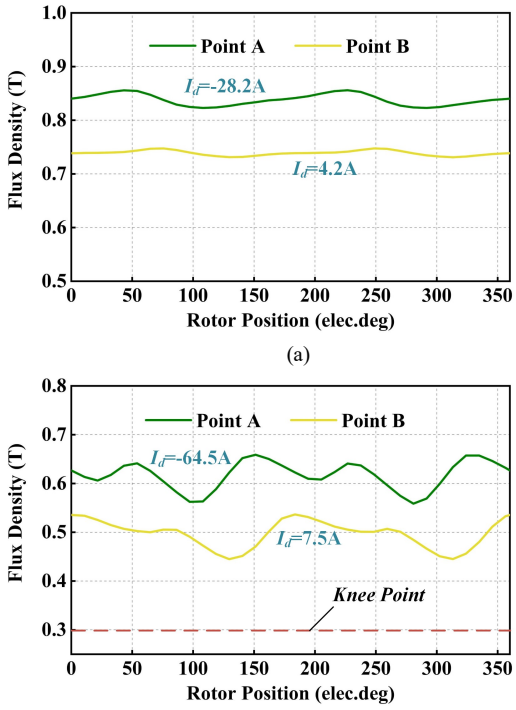

Fig. 17. Flux density variation of observation PM points of the two machines at different rotor positions. (a) Rated current condition. (b) Over loaded current condition.

maximum output torque are applied as the basis for testing whether the PMs will be demagnetized. Under the rated current condition, the current angle for maximum torque of the conventional IPM machine is 36°, where the d-axis current is -28.2A, and the current angle for maximum torque is 42.2° under the double-rated current condition, where the d-axis current is -64.5A. Due to the intensifying-flux effect of the IFVF-IPM machine, the maximum torque can be generated when the current angle for maximum torque is negative, leading the d-axis current is 4.2A and the current angle is -5° when the rated current is applied. Similarly, d-axis current is 7.5A and the current angle is -4.5°when twice the rated current is applied.

The experimental results are shown in the Fig.17. It is found that the flux density of point A and point B is keep in high condition as shown in Fig.17(a) when rated current is applied, which means that the two machines have low risks of demagnetization. Fig.17(b) is the experimental results of two observation points when twice the rated current is applied, and the knee point of irreversible demagnetization risk is about 0.3T for the limit operating temperature 150°C from the BH curve of PMs (N38SH). Obviously, both conventional IPM machine and the proposed IFVF-IPM machine have no risk of irreversible demagnetization, while the flux density of the PMs of the two machines are much higher than knee point.

And the risk of the irreversible demagnetization in the flux weakening region at the speed of 5000r/min is also be investigated. Both machines are operating in flux weakening region, and the d-axis current with demagnetization properties are -46.5A and -38.1A respectively. The flux density of the proposed IFVF-IPM machine is higher than conventional IPM machine in flux weakening region as shown in Fig.18, which indicates that the risk of irreversible demagnetization can also be reduced for proposed IFVF-IPM machine which represents a better performance to resist demagnetization risks.

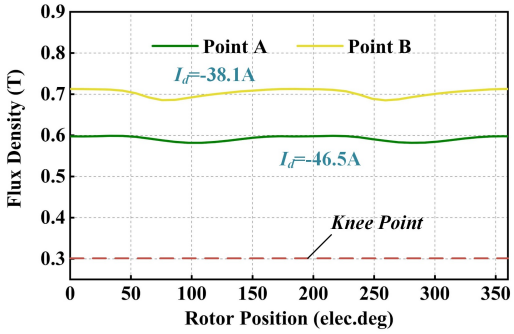

Fig. 18. Flux density variation of observation PM points of the two machines in flux weakening region at different rotor positions.

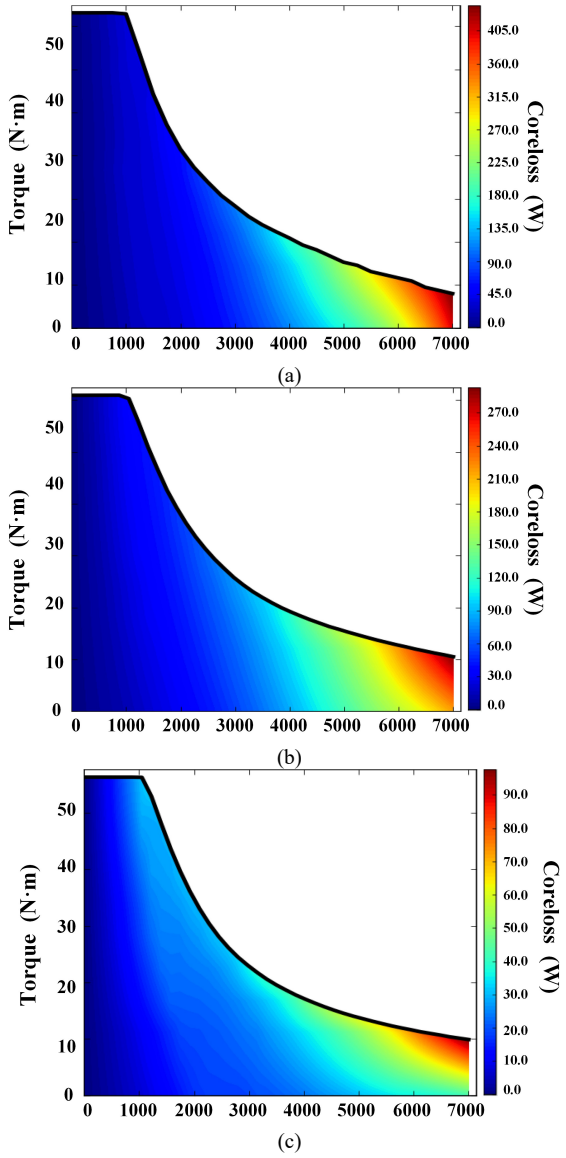

Fig. 19. Core loss of three machines. (a) Conventional IPM machine. (b) CIFVF-IPM machine. (c) IFVF-IPM machine.

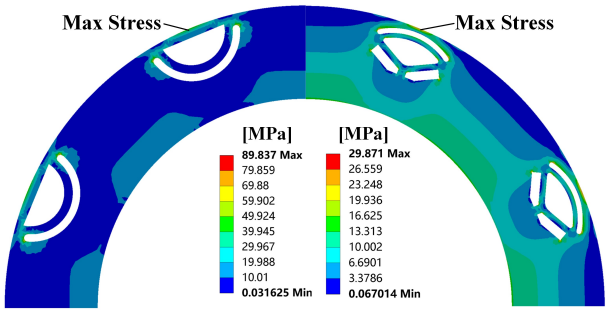

(a) (b)

Fig. 20. Stress analysis of two machines. (a) Conventional IPM machine. (b) IF-VF IPM machine.

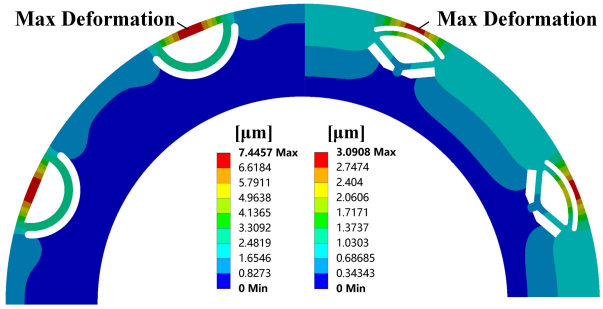

(a) (b)

Fig. 21. Max deformation of two machines. (a) Conventional IPM machine. (b) IF-VF IPM machine.

E. Core Loss Comparison

Theoretically, flux density in core of IFVF-IPM machines is smaller compared with the conventional IPM machine in flux weakening region which are caused by variable flux-leakage characteristics, which will leads less core loss. FEA result shown in Fig. 18 characterizes the core loss map of the three machines at different speeds, and the given maximum speed is 7000r/min. When the speed reaches the given maximum, the core loss of the conventional IPM machine is 405W, while the core loss of the CIFVF-IPM machine and the IFVF-IPM machine are 270W and 90W respectively, we can see that the core loss is greatly reduced in proposed IFVF-IPM machine, this is because the q-axis current is reduced which leads the flux leakage path not saturated when operating in flux weakening region, so a large amount of flux leakage is generated, and the magnetic flux in the iron core is reduced, hence, the feasibility of reducing the core loss by varying the flux leakage is verified.

F. Deformation and Stress Analysis

In the design of the magnetic circuit of the proposed IFVF-IPM machine, the intensifying flux effect and the characteristics of variable flux leakage are achieved by setting the flux barriers, which will reduce the machinal strength. Therefore, the analysis of deformation and stress of the rotor are necessary when the machine operating at high speeds. The influence of electromagnetic force is so small compared with radial force that can be ignored, and the deformation and stress of the rotor is mainly analyzed. Fig. 19 shows the mechanical stress analysis results, the maximum stress points of the two motors have been marked in the figure which are 89.837MPa and 29.871Mpa, respectively, both are within the reasonable allowable range.

In addition, we also analyzed the deformation of the rotors at 10000r/min in Fig.20, which are 7.4457μm and 3.0908μm, respectively. The deformation of the IFVF-IPM machine is smaller than that of the conventional IPM machine, which reflects the higher machinal reliability.

V. CONCLUSIONS

A novel intensifying-flux machine with the characteristics of L_d>L_q is proposed in this paper, in which the flux leakage is controllable. The FEA method is used to evaluate the proposed machine and the electromagnetic performances of IFVF-IPM machine indicates that:

(1) Effectiveness and feasibility of rotor structure design that including three parallel leakage flux paths which can increase the variable flux range, thus enhance the ability of flux weakening and reduce the core loss.

(2) The proposed IFVF-IPM machine has a better flux weakening capability with variable flux-leakage, which means a wider speed range.

(3) The IFVF-IPM machine has a lower risk of irreversible demagnetization and less iron loss.

REFERENCES

[1] Dalal, Ankit, and P. Kumar. “Design, Prototyping and Testing of Dual Rotor Motor for Electric Vehicle Application.” *IEEE Transactions on Industrial Electronics*, vol. 65, no. 9, pp. 7185 – 7192, Sept. 2018.

[2] Aljehaimi, Akrem M, and P. Pillay. “Operating Envelopes of the Variable Flux Machine with Positive Reluctance Torque.” *IEEE Transactions on Transportation Electrification,* vol. 4, no.3, pp. 707-719, Sept. 2018.

[3] K. Akatsu, M. Arimitsu , and S. Wakui. “Design and Control of a Field Intensified Interior Permanent Magnet Synchronous Machine.” *IEEE Transactions on Industry Applications*, vol. 126, no. 7, pp. 827-834, 2015.

[4] Zhu, X., et al. “Comparative Design and Analysis of New Type of Flux-Intensifying Interior Permanent Magnet Motors with Different Q-Axis Rotor Flux Barriers”, *IEEE Transactions on Energy Conversion*, vol. 33, no. 4, pp. 2060-2069, Dce. 2018.

[5] Yang, et al. “Electromagnetic Performance Analysis and Verification of a New Flux-Intensifying Permanent Magnet Brushless Motor with Two-Layer Segmented Permanent Magnets”, *IEEE Transactions on Magnetics*, vol. 52, no. 7, 2016.

[6] X. Zhu, et al. “Comprehensive Sensitivity Analysis and Multi-Objective Optimization Research of Permanent Magnet Flux-Intensifying Motors”, *IEEE Transactions on Industrial Electronics,* vol. 66, no. 4, pp. 2613-2627, April, 2019.

[7] N. Limsuwan, et al. “Novel Design of Flux-Intensifying Interior Permanent Magnet Synchronous Machine Suitable for Self-Sensing Control at Very Low Speed and Power Conversion”, *IEEE Transactions on Industry Applications*, vol. 47, no. 5, pp. 2004-2012, Sept.-Oct. 2011.

[8] T. Kato, et al. “Design Methodology for Variable Leakage Flux IPM for Automobile Traction Drives.” *IEEE Transactions* on *Industry Applications*, vol. 51, no. 5, pp. 3811-3821, 2014.

[9] N. Limsuwan, T. Kato, K. Akatsu, et al. “Design and Evaluation of a Variable-Flux Flux-Intensifying Interior Permanent-Magnet Machine”, *IEEE Transactions on Industry Applications*, vol. 50, no. 2, pp. 1015-1024, 2014.

[10] Lei Xu, Xiaoyong Zhu, Wenye Wu, et al., “Flux-Leakage Design Principle and Multiple-Operating Conditions Modeling of Flux Leakage Controllable PM Machine Considering Driving Cycles”, *IEEE Transactions on Industrial Electronics*, vol. 69, no. 9, pp. 8862-8874, Sept. 2022.

[11] W. Wu, Y. Sun, Y. Wu, S. Zong and W. Wu, “Design and Analysis of Adjustable Flux Leakage Characteristics in IPM Synchronous Machine Based on Regression Orthogonal Method”, in Proc. *2020 IEEE International Conference on Applied Superconductivity and*

Electromagnetic Devices (ASEMD), Tianjin, China, 2020, pp. 1-2.

[12] Dutta, R., and M. F. Rahman. "Design and Analysis of an Interior Permanent Magnet (IPM) Machine with Very Wide Constant Power Operation Range", *IEEE Transactions on Energy Conversion*, vol. 23, no. 1, pp. 25-33, Mar. 2008.

[13] X. Sun, Z. Shi, G. Lei, Y. Guo, and J. Zhu, "Multi-Objective Design Optimization of an IPMSM Based on Multilevel Strategy," in *IEEE Transactions on Industrial Electronics*, vol. 68, no. 1, pp. 139-148, Jan. 2021.

[14] K. Diao, X. Sun, G. Lei, Y. Guo, and J. Zhu, "Multi-objective System Level Optimization Method for Switched Reluctance Motor Drive Systems Using Finite-Element Model," in IEEE Transactions on Industrial Electronics, vol. 67, no. 12, pp. 10055-10064, Dec. 2020

Xiping Liu received his B.S. degree from Hohai University, Nanjing, China, in 1999; his M.S. degree from the Jiangxi University of Science and Technology, Ganzhou, China, in 2004; and his Ph.D. degree in Electrical Engineering from Southeast University, Nanjing, China, in 2009. He is presently working as a Professor in the Department of Electrical Engineering and Automation, Jiangxi University of Science and Technology. His current research interests include the analysis and design of permanent magnet synchronous machine, and wind power technology.

Dabin Liu was born in China in 1994, he received his B.S. degree from Nanchang University, Nanchang, China, in 2015; He is presently working toward his M.S. degree in Electrical Engineering at the Jiangxi University of Science and Technology, Ganzhou, China. His current research interests include the design of permanent magnet motors, the interior PMSMs and their control method.

Siting Zhu was born in China, in 1996, she received her B.S. degree from Jiangxi University of Science and Technology, Ganzhou, China, in 2016. She is presently working towards her M.S. degree in Electrical Engineering at Jiangxi University of Science and Technology. Her current research includes design and analysis of PMSMs, and the intensifying-flux of variable leakage flux PMSMs.

Jianwei Liang was born in China. He received his B.S. degree from Jiangxi University of Science and Technology, Ganzhou, China; his M.S. degree from the Nanchang University, Nanchang, China. He is presently working as an Associate Professor at the Jiangxi University of Science and Technology. His current research interests include PMSMs, and their drive and control.